Petroleum Science 22 (2025) 1360–1369

Contents lists available at ScienceDirect

Petroleum Science

journal homepage: www.keaipublishing.com/en/journals/petroleum-science

Original Paper

Study on the mass transfer characteristics of hydrogen in heavy oil by a modified dynamic pressure step method

Tao Jiang [a], Fei Yu [a], Qian-Min Jiang [a], Yan-Xin Song [a], Qing-Feng Tan [b], Wu Su [b], Xu Yang [b], Zhen-Tao Chen [a, *], Chun-Ming Xu [a]

[a] State Key Laboratory of Heavy Oil Processing, China University of Petroleum, Beijing, 102249, China
[b] Petrochemical Research Institute, PetroChina Company Limited, Beijing, 102206, China

ARTICLE INFO

Article history:
Received 3 February 2024
Received in revised form
20 August 2024
Accepted 29 September 2024
Available online 30 September 2024

Edited by Min Li

Keywords:
Hydrogenation
Heavy oil
Hydrogen solubility
Gas-liquid mass transfer

ABSTRACT

The dissolved hydrogen, rather than gaseous hydrogen, plays a crucial role in the hydrogenation process. A thorough understanding of hydrogen dissolution is essential for optimizing the hydrogenation process. In this paper, the dynamic pressure step method was modified to reduce the temperature difference between the hydrogen and solution, from which the hydrogen solubility and volumetric liquid-side mass transfer coefficient (k_La) of the vacuum residue were obtained. It was discovered that temperature was the most critical factor in hydrogen dissolution, simultaneously enhancing both the hydrogen solubility and k_La. Pressure played a significant role in promoting hydrogen solubility, but had a relatively small impact on k_La. Stirring speed, although it enhanced k_La, did not affect hydrogen solubility. By normalizing the dissolution parameter, the results showed that the gas-liquid mass transfer rate decreased continuously during hydrogen dissolution and that the S_D-t_D curves after normalization were almost the same in all experimental conditions.

1. Introduction

The declining availability of conventional crudes is leading to increased utilization of heavy crudes or residua in refineries to meet the demand for valuable products. These heavy feedstocks contain high levels of sulfur, nitrogen, and contaminant metals, which can cause catalyst deactivation in consequent processes and pose serious environmental hazards (Chen et al., 2010; Jiménez et al., 2007; Mapiour et al., 2010b). Hydrotreating is an essential process in refineries for upgrading heavy oil and residue, which substantially reduces the level of impurities and provides a large quality of high-quality feedstocks for downstream conversion units (Baird et al., 2017; Rana et al., 2007).

Hydrotreating technology has developed rapidly over the past two decades, primarily due to a better understanding of reaction chemistry and kinetics. Extensive research has shown that the operating conditions significantly influence the hydrotreating (HDT) reaction, including temperature, H_2 partial pressure, H_2/oil ratio, and liquid hourly space velocity (LHSV). Increasing hydrogen pressure has been found to have a substantial impact on the hydrotreatment of residual oil, increasing the rates of hydrodemetallization (HDM) and hydrodesulfurization (HDS) reactions and enhancing catalyst life (Al-Mutairi and Marafi, 2012). To increase hydrogen partial pressure, one can adjust the total pressure, gas/oil ratio, or hydrogen purity. Similar positive effects of these operational variables have also been observed for HDS, hydrodenitrogenation (HDN), and hydrodearomatization (HAD) (Mapiour et al., 2009). Generally, the results of pressure, hydrogen purity, and gas/oil ratio can all be attributed to hydrogen partial pressure, although the exact mechanism is unclear. Furthermore, while researchers often consider the simulating effect of temperature on hydrotreatment due to its influence on intrinsic reactivity and diffusional resistance reduction (Callejas and Martínez, 2000; Wang et al., 2014), the promoting effect from the perspective of hydrogen dissolution has been seldom elucidated.

Residue HDT involves three phases: gas, liquid, and solid. In this process, catalysts facilitate the addition of hydrogen to the residues. It is important to note that active hydrogen participates in the reaction rather than gaseous hydrogen. For the hydrogen to react, it must diffuse across the gas-liquid interface and reach the active site

* Corresponding author.
E-mail address: czt@cup.edu.cn (Z.-T. Chen).

https://doi.org/10.1016/j.petsci.2024.09.026

of the catalyst along with the residue molecules. The hydrogen diffusion rate at the gas-liquid interface is relatively slow, often becoming a rate-limiting step in residue HDT. Therefore, the solubility of hydrogen and the gas-liquid mass transfer in residues under operational conditions are the key factors that affect the hydrogenating efficiency (Wang et al., 2021). These factors are critical for properly optimizing process operations and designing a suitable reactor (Florusse et al., 2003; Ronze et al., 2002; Sebastian et al., 1981; Shaharun et al., 2008).

While researchers have recognized the significant importance of hydrogen transfer in the hydrotreating processes, the optimization of hydrogen usage in the residue HDT is still in need of improvement due to insufficient knowledge of the gas-liquid mass transfer. Since a substantial amount of hydrogen is consumed in the residue HDT, maintaining sufficient hydrogen dissolved in the liquid phase is crucial to ensure effective hydrogen activation on the catalyst surface. Most kinetic studies on HDT indicate that operations are conducted with excess hydrogen (Wang et al., 2018). The hydrogen-to-oil ratio is typically specified at a minimum of three or four times the expected hydrogen consumption to facilitate optimal mass transfer between reactants and catalyst and prevent catalyst deactivation caused by coke formation (Hoekstra, 2007; Pinos et al., 2019). However, it is essential to note that excessive hydrogen can lead to energy waste, high processing costs, and potential safety hazards. Therefore, it's necessary to study the solubility and gas-liquid mass transfer in heavy oil-hydrogen systems to optimize the hydrotreating process and ensure efficient hydrogen utilization.

Hydrogen solubility in liquid materials has primarily been studied using direct sampling methods (Cai et al., 2001a; Lal et al., 1999; Ronze et al., 2002) and indirect calculating methods (Baird et al., 2017; Saajanlehto et al., 2014b; Uusi-Kyyny et al., 2017). All experimental results confirmed that hydrogen solubility in oils gradually increases with temperature and pressure (Cai et al., 2001b; Ji et al., 2013; Riazi and Vera, 2004; Saajanlehto et al., 2014a). The decrease in hydrogen solubility in heavy oils follows the pattern observed in pure solvents: saturated hydrocarbon > aromatics > non-hydrocarbon compounds, and the hydrogen solubility increases as the carbon length of the alkanes increases and the number of aromatic rings decreases (Brunner, 2002; Luo et al., 2010). Moreover, the hydrogen solubility decreases with increasing asphaltene content of heavy oil (Bai et al., 2019). Unfortunately, the thermal instability of heavy oils at high temperatures and pressures, coupled with their low hydrogen solubility, makes accurate experimental measurements very challenging (Krishnamurthy et al., 2006; Saajanlehto et al., 2014a).

Currently, the hydrotreating of heavy petroleum and residue will continue to increase in importance as worldwide trends in crude oil supply have been shifting to heavier feedstocks. For residue hydrotreatments, the overall reaction rate is significantly limited by the transport of hydrogen from the hydrogen-residue interface to the bulk liquid. The transport is proportional to the product volumetric liquid-side mass transfer coefficient (k_La). The k_La values can be determined in an autoclave by the physical absorption method (specifically, the dynamic pressure-step method), and they are influenced by temperature, pressure, and stirring speed. However, available information is scarce in the literature regarding the effects of these factors on k_La, which highlights the ongoing controversy surrounding the effect of pressure and temperature on k_La (Tekie et al., 1997). Furthermore, previous studies have mostly focused on measurements under relatively mild conditions (pressure <5 MPa, temperature <427 K) and the temperature difference between the gas and liquid phases leads to large measurement errors (Chang and Morsi, 1991; Heintz et al., 2009; Inga and Morsi, 1997; Koneripalli et al., 1994; Larachi et al., 1998; Lei et al., 2016; Sharma et al., 2009; Teramoto et al., 1974; Zhang et al., 2014; Zieverink et al., 2006). The properties of heavy oil, such as high viscosity and low mass transfer rate, make it challenging to obtain accurate mass transfer data for hydrogen in heavy oil under elevated temperature and pressure.

The primary focus of this paper is to obtain accurate data on hydrogen solubility and the gas-liquid mass transfer coefficient in vacuum residue under close-to-process conditions using a modified dynamic pressure step method. We investigated the effects of temperature, pressure, and stirring speed on hydrogen solubility and volumetric liquid-side mass transfer coefficient through comparative analysis. Furthermore, the amount of dissolved hydrogen and the corresponding time for all conditions were normalized to examine the variation in mass transfer rate. This analysis provides valuable insight into the hydrotreating conversions from the perspective of hydrogen supply. To the best of our knowledge, previous investigations have not reported dynamic data or mass transfer coefficients regarding hydrogen dissolution in residue.

2. Experimental section

2.1. Materials

The purity of hydrogen was 99.999% from Beijing AP Baif Gases Industry Co., Ltd. Hexadecane was supplied by Shanghai Aladdin Bio-Chem Technology Co. Vacuum residue (VR) was provided by Petrochemical Research Institute (PRI) of PetroChina Company Limited, and its main properties are listed in Table 1.

To account for the high viscosity of PRI-VR, densities were determined by the specific gravity bottle method at a temperature range of 373.15–473.15 K and atmospheric pressure. The obtained density values are listed in Table 2. The density-temperature (ρ-T) curve was fitted using a simple correlation according to the data points, resulting in Eq. (1). The correlation coefficient R^2 was 0.99993.

$$\rho = -0.000486676T + 1.14116 \quad (1)$$

2.2. Experimental setup and procedure

The hydrogen dissolution experiments were conducted using a modified dynamic pressure step method. The schematic diagram of the experimental setup is shown in Fig. 1. The experimental setup mainly consisted of three parts: a hydrogen preheating system (A_1), a hydrogen dissolution system (A_2), and a data acquisition system. The key equipment in A_1 and A_2 was the stirred autoclave. Preheated hydrogen from A_1 was charged into A_2 for the hydrogen dissolution experiments, and dynamic data of pressure in A_2 was collected to calculate the hydrogen solubility and k_La value. A_2, purchased from Top Industrie France (model TOP 60), was designed to safely operate at pressure up to 2000 bar and temperatures up to

Table 1
Physical and chemical properties of VR.

Item	PRI-VR	Item	PRI-VR
Density at 100 °C, g/cm^3	0.9594	IBP, °C	401.8
Viscosity at 100 °C, mPa/s	414.83	30%, °C	534.2
Molecular weight	1042	70%, °C	622.2
C, wt%	85.64	FBP, °C	745.4
H, wt%	10.88	Saturates, m%	19.93
S, wt%	0.02	Aromatics, m%	49.78
N, wt%	0.41	Resin, m%	24.30
H/C atomic ratio	1.52	Asphaltene, m%	5.98

Table 2
Densities of PRI-VR at different temperatures.

Temperature T, K	373.15	393.15	413.15	433.15	453.15	473.15
Density ρ, g/cm^3	0.9594	0.9495	0.9405	0.9302	0.9207	0.9109

600 °C. A standard six-bladed Rushton disc impeller was used to mix the solution in A_2, as shown in Fig. 2. The volumes of the autoclaves were measured using the water replacement method and were determined to be 500 mL. Temperature measurements were obtained using a movable axial thermocouple (accuracy of 0.1 °C) positioned inside the autoclave. The pressure was measured using a transducer (model MDM3051S-GPHH-A3N11D, accuracy 0.01 MPa) from Mack Sensors Co.

The pipeline connecting the two autoclaves was insulated with heating tape to minimize heat loss during the transportation of preheated hydrogen. Instead of using a separate preheater, a volumetric autoclave A_1 was employed. The temperature of A_1 was set higher than that of A_2 to compensate for any heat loss during the hydrogen flow and ensure precise temperature control of the gas and liquid phases within A_2.

The experimental procedure was briefly described as follows: a liquid feedstock with a mass of m_L was loaded into A_2. After sealing, it was purged with N_2 and pressurized to 10.0 MPa at room temperature. A leak test was conducted for 1 h. Subsequently, A_2 was degassed for 1 h with a stirring speed of 600 r/min and a temperature of 120 °C. The heating process began with high-speed stirring until the desired experimental temperature T_e was reached. Meanwhile, a specific amount of hydrogen was charged into A_1 at room temperature and heated to the preheating temperature T_h. The preheated hydrogen was then introduced into A_2. Stirring in A_2 commenced once the pressure achieved a steady state (P=P_i), and the pressure in A_2 was recorded over time until thermodynamic equilibrium was reached (P=P_e). Hydrogen solubility and k_La values were calculated using the dynamic pressure data. All experiments were performed in triplicate, and excellent reproducibility was achieved under identical process conditions.

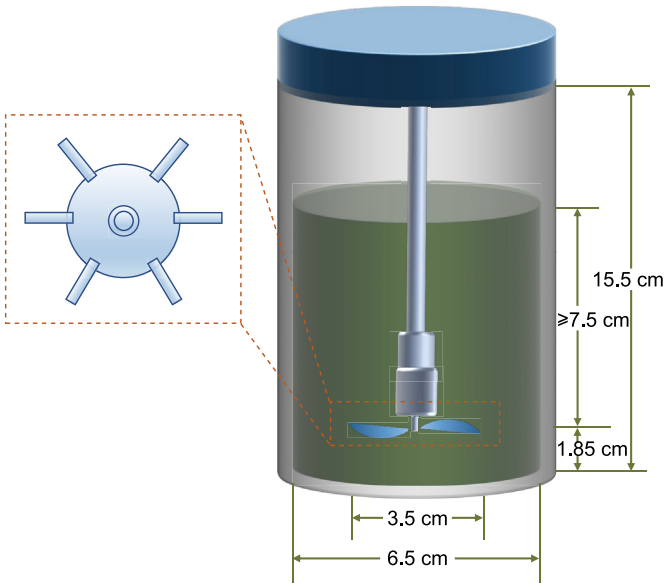

Fig. 2. Structure and dimensions of hydrogen dissolution autoclave and impeller.

It should be noted that the amount of hydrogen at room temperature in A_1 can be estimated using the ideal gas law, as the volumes of the autoclaves and pipelines were determined. Furthermore, the preheating temperature in A_1 was determined through prior repeated tests, and the optimum values are listed in Table 3. The table indicates that the compensation temperature (T_C), which is the temperature difference between the A_1 and A_2, increases with higher temperatures and pressures. The temperature of A_1 was set to T_h according to the target value for the hydrogen dissolution experiment.

In this study, the uncertainty of hydrogen solubility and k_La mainly depends on the temperature and pressure. The measurement accuracy of the temperature and pressure sensor is 0.1 °C and

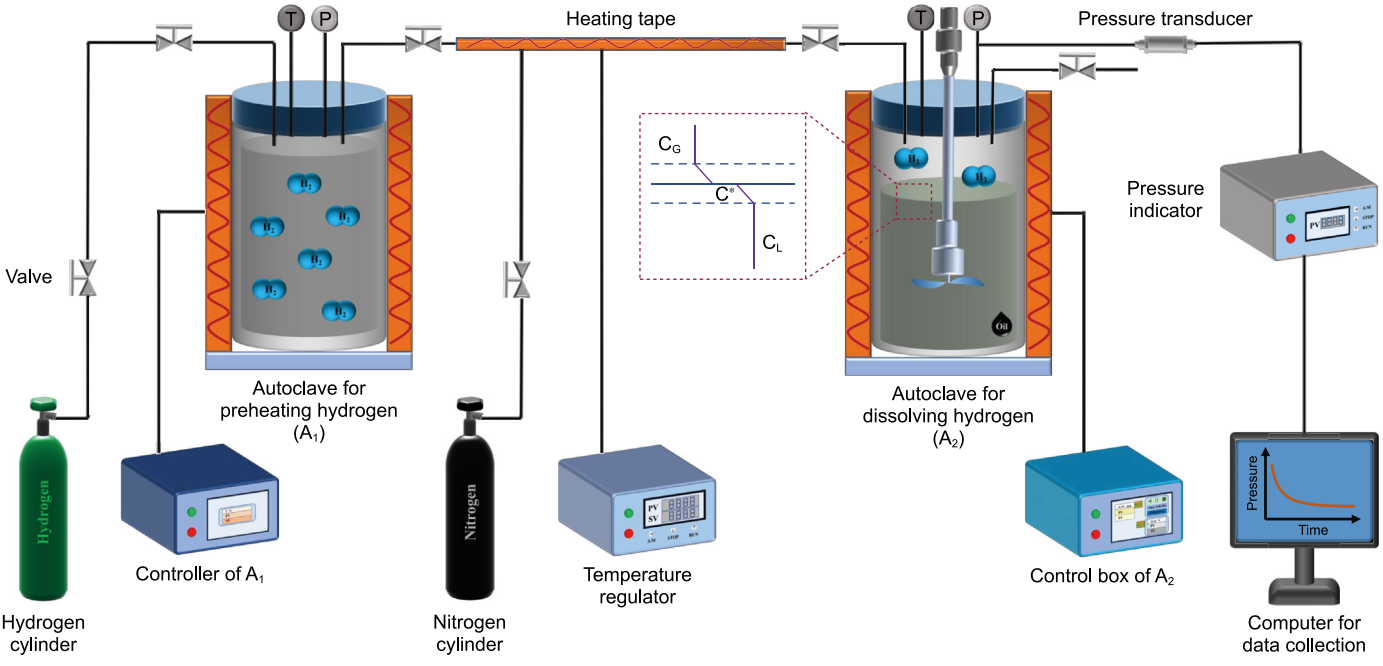

Fig. 1. Schematic diagram of the experimental setup.

Table 3
Results of T_C at some experimental conditions.

T, K	P, MPa	T_C, K	T, K	P, MPa	T_C, K
513.15	5.812	5.2	553.15	5.853	6.7
513.15	6.680	5.5	553.15	7.070	7.2
513.15	8.174	5.9	553.15	8.409	8
533.15	5.638	5.8	573.15	5.638	7.5
533.15	7.345	6.4	573.15	7.048	8.5
533.15	8.763	7	573.15	8.195	9.6

0.01 MPa, respectively. The fluctuation range of the temperature is ±0.5 °C during the experiment. The corresponding error was analyzed and provided along with the experimental results.

2.3. Hydrogen solubility(S) and volumetric liquid-side mass transfer coefficient (k_La)

The solubility of hydrogen in liquids was obtained from the beginning and ending points of the *P-t* curve based on the principle of isovolumetric absorption. The moles of hydrogen N_L dissolved in the liquid can be calculated by the following Equation:

$$N_L = \frac{V_G P_i}{Z_i R T_e} - \frac{V_G P_e}{Z_e R T_e} \tag{2}$$

where V_G is the volume of the gas phase in A_2. Z_i and Z_e are the compressibility factors at P_i and P_e, respectively, which were calculated by the PR equation of state. Since the vapor pressure of the residue was negligible, the hydrogen solubility S can be calculated by Eq. (3).

$$S = \frac{N_L}{\frac{m_L}{1000}} \tag{3}$$

The k_La values were obtained from the transient part of the *P-t* curve by the dynamic pressure step method. The following Equation can calculate the rate of pressure variation:

$$\frac{dP}{dt} = \frac{ZRT}{V_G}\frac{dN_G}{dt} = -\frac{ZRT}{V_G}\frac{dN_L}{dt} \tag{4}$$

where N_G is the reduced molar amount of hydrogen in the gas phase. The gas-phase mass transfer resistance was negligible, and the rate of gas-liquid mass transfer can be calculated by Eq. (5) based on the two-film theory.

$$\frac{dC_L}{dt} = k_L a(C^* - C_L) \tag{5}$$

where C^* and C_L are the equilibrium concentration of hydrogen in the liquid and the hydrogen concentration in the liquid, respectively. Eq. (6) can be obtained by using Henry's law and the integral form of Eq. (4).

$$\frac{dP}{dt} = k_L a[(\alpha+1)P - P_i - \alpha P_0] \tag{6}$$

where

$$\alpha = \frac{V_L}{V_G}\frac{RT}{H} \tag{7}$$

where H is Henry's constant. Eq. (8) was obtained by integrating Eq. (6) between $t_0 = 0$ (P=P_i) and t (P=P_e). The polynomial of pressure was proportional to time, and the scale factor was the k_La value.

$$\frac{P_e}{P_i}\ln\left(\frac{P_i - P_e}{P - P_e}\right) = k_L a(t - t_0) \tag{8}$$

In the early stage of hydrogen dissolution, it took some time for the gas-liquid phase to reach a stable hydrodynamic state. In the later stage, the pressure drop was so small that the temperature fluctuations could influence the pressure in A_2. Considering the transition to a steady stirring state and the effects of temperature fluctuations, the *P-t* curve section from $t = 50$ s to 80% of the total pressure drop was used to determine the k_La values.

2.4. Normalization process

The variation of mass transfer rate can be obtained from the dynamic data of hydrogen dissolution in residue. In Eq. (5), the k_La and C^* values are constant, and therefore, C_L becomes the sole factor influencing the mass transfer rate under specific conditions. The study of the mass transfer rate can be simplified by focusing on C_L. C_L changes with time t, while C^* and t^* (equilibrium time) vary with the operating conditions. To assess the variation in gas-liquid mass transfer rates, the normalization of C_L and t is proposed to achieve a universal understanding of the hydrogen dissolution process. Furthermore, to easily understand the subsequent analytical discussion, C^* is denoted as S, as C^* represents an expression of S. As a result of the above treatment, two dimensionless parameters, S_D and t_D, can be obtained from Eqs. (9) and (10).

$$S_D = \frac{C_L}{S}{}^*100\% = \frac{C_L}{C^*} \times 100\% \tag{9}$$

$$t_D = \frac{t}{t^*} \times 100\% \tag{10}$$

where S_D and t_D are the normalizations of hydrogen concentration and dissolution time in the solution, respectively. It is evident that the S_D-t_D curve reflects the behavior observed in the *P-t* curve, and the slope of the curve is proportional to the mass transfer rate.

2.5. Reliability verification of experimental setup and operation method

To verify the reliability of the experimental apparatus and the modified method, the hydrogen solubility in hexadecane was determined in the pressure range of 1–10 MPa and temperature range of 453.15 and 543.15 K. The results, shown in Fig. 3, were compared with those in the literature (Luo et al., 2010). The comparison revealed a good agreement between the hydrogen solubility obtained in this study and the previously reported values under similar conditions, indicating the reliability of the established apparatus and the modified method for hydrogen solubility measurement. Furthermore, a slight deviation was observed in some of the data from Luo (Luo et al., 2010), suggesting that the apparatus's modifications had improved the measurement's accuracy.

3. Results and discussion

This study investigated hydrogen solubility and gas-liquid mass transfer in PRI-VR under the following conditions: temperature range of 240–320 °C, pressure range of 4–9 MPa, and stirring speed range of 300–600 r/min. The lower limit of the temperature range was determined by the viscosity of PRI-VR, while the upper limit was constrained by the thermal and hydrogenation stability of PRI-VR.

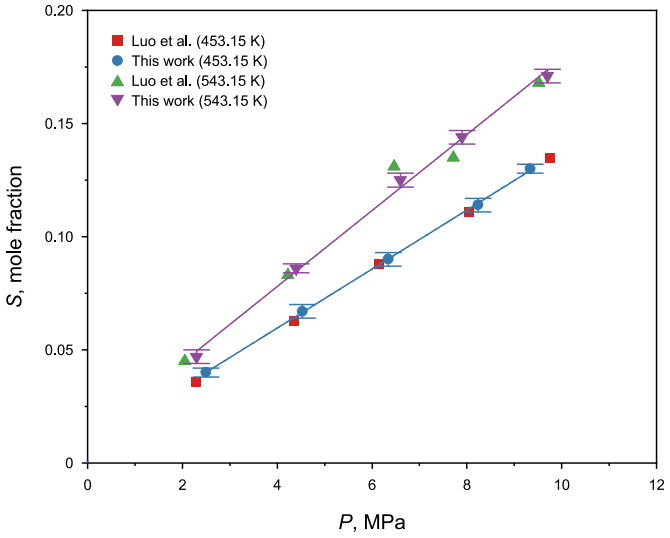

Fig. 3. Comparison of H_2 solubility in hexadecane between experimental data obtained in this work and those in the literature (Luo et al., 2010).

3.1. Hydrogen solubility

Experimental data for the hydrogen solubility in PRI-VR are illustrated in Fig. 4. As shown in Fig. 4(a), the solubility of hydrogen increases with temperature and pressure at the stirring speed of 600 r/min. At the same temperature, the solubility of hydrogen at 9 MPa was almost twice as much as that at 4 MPa. The solubility of hydrogen increased by about one-third when the temperature increased from 240 to 320 °C at the same pressure. The relationship between the solubility of hydrogen and pressure follows a linear trend, which is typical in gas-liquid systems containing hydrogen (Ding et al., 1985; Lei et al., 2014; Tsuji et al., 2005). The "inverse" temperature effect observed in common solvents is attributed to the positive excess enthalpy in the hydrogen-solvent interaction (Lei et al., 2016). According to Henry's law, dissolved hydrogen is directly proportional to its partial pressure. Since the vaporization of PRI-VR is negligible, the partial pressure is equal to the total pressure. Thus, the results of this study seem reasonable and consistent with the findings in the literature (Cai et al., 2001a; Ji et al., 2013; Lal et al., 1999; Saajanlehto et al., 2014a). Previous studies have also indicated that the presence of large amounts of aromatics and non-hydrocarbons in oils can decrease hydrogen solubility, and the solubility of hydrogen in aromatic hydrocarbons decreases as the number of aromatic rings increases (Brunner, 2002; Park et al., 1996). Therefore, the lower solubility of hydrogen observed in this work compared to the literature can be attributed to the high content of polycyclic aromatic hydrocarbons, resins, and asphaltenes in PRI-VR.

Fig. 4(b) shows that the hydrogen solubility of PRI-VR remains unaffected by stirring speed within the range of 300–600 r/min, which indicates that the solubility is determined by thermodynamic equilibrium.

Temperature and pressure are the primary factors influencing the solubility of hydrogen. In the hydrotreating of heavy oil, pressure refers to the hydrogen partial pressure, which is influenced by temperature, pressure, gas/oil ratio, H_2 purity, and LHSV (Mapiour et al., 2010a). Experimental results by Mapiour showed that the pressure and hydrogen purity had a more significant impact on HDS, HDN, and HDA than the gas-oil ratio in the trickle-bed reactor. However, temperature and LHSV had little effect on the hydrogen partial pressure (Mapiour et al., 2010b). Higher temperatures or pressures result in increased hydrogen dissolution in the feedstock, making more hydrogen available on the catalyst surface for the hydrotreating reaction. The enhanced hydrogenating efficiency at elevated temperature and pressure can be attributed, in part, to the improved hydrogen solubility.

3.2. The regime of gas-liquid mass transfer

Understanding the flow regimes is essential for gas-liquid mass transfer. Albal et al. (1983) classified gas-liquid mass transfer into three types based on the effect of stirring speed on the surface of the liquid, while Kara et al. (1983) divided the effect of stirring speed on k_La into two regions. The critical stirring speed was used to define the regimes of the mass transfer and was determined by the stirring speed at which the k_La value increases sharply (Kara et al., 1983). When the stirring speed exceeds the critical value, the liquid surface begins to break, gas becomes entrained in the liquid, and the k_La is significantly affected by agitation. This study investigated the effect of stirring speed on k_La at stirring speeds of 300–600 r/min, pressures of 8.5 MPa, and temperatures of 240–320 °C. As shown in Fig. 5, the k_La value increases exponentially with increasing stirring speed, indicating that the stirring speed is above the critical value, and gas-liquid mass transfer occurs at the liquid surface and hydrogen bubble walls, respectively. After reaching dissolution equilibrium, the stirrer was switched off, and a slight increase in pressure in A_2 was observed, further confirming that the stirring speed exceeded the critical value. However,

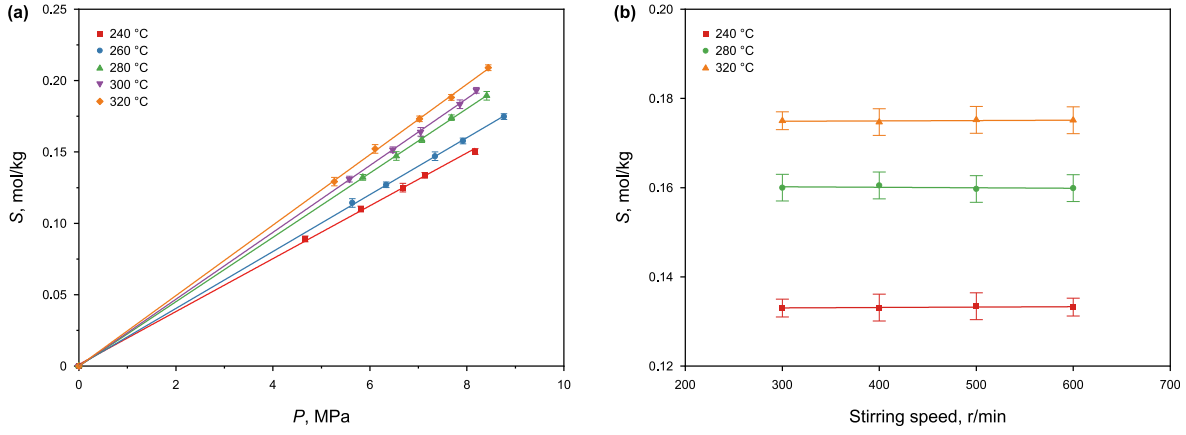

Fig. 4. Hydrogen solubility C*: **(a)** at 600 r/min, **(b)** at different stirring speeds and 7 MPa.

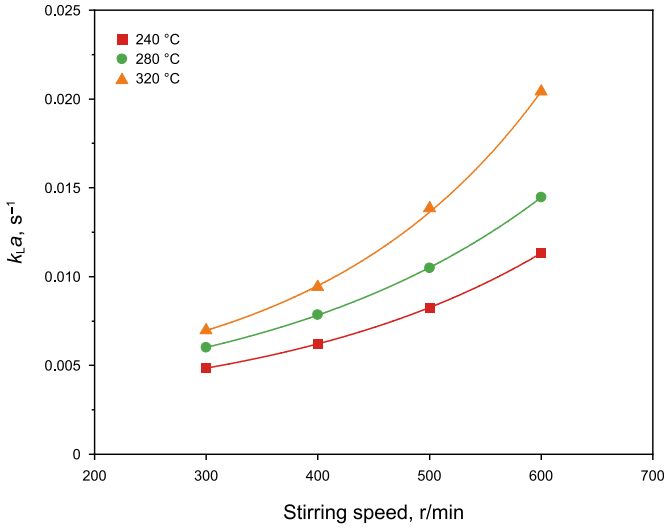

Fig. 5. Volumetric liquid-side mass transfer coefficient k_La at different stirring speeds and 7 MPa.

since the impeller was positioned far from the liquid surface (more than 10 cm), the gas entrainment rate was low. As a result, the pressure increase was minimal and did not affect the calculation of hydrogen solubility.

3.3. Volumetric liquid-side mass transfer coefficient

3.3.1. Effect of stirring speed on k_La

Fig. 5 illustrates the effect of stirring speed on k_La. The k_La values exhibit an exponential increase with increasing stirring speed at a given temperature and pressure, especially at higher temperatures. The finding of this study demonstrates a reasonable agreement with the literature (Albal et al., 1984; Chang et al., 1991; Koneripalli et al., 1994).

Fig. 6 presents the effect of stirring speed on gas-liquid mass transfer and temperature of PRI-VR. At low stirring speeds (<300 r/min), the turbulent kinetic energy required for the complete dispersion of hydrogen and PRI-VR is insufficient. This leads to a higher concentration of hydrogen near the gas-liquid interface, resulting in a slight difference in hydrogen concentration between the two sides of the gas-liquid interface and a low gas-liquid mass transfer rate. Therefore, it was found that when the stirring speed was 100 r/min, the pressure in A_2 hardly changed and the k_La value was close to zero. From the relationship between k_La value and stirring speed, it can be inferred that the critical stirring speed is between 100 and 300 r/min. As the stirring speed increases, the contact between hydrogen and liquid is intensified and the mixedness of the liquid is enhanced. When the stirring speed is high enough, the hydrogen concentration in the liquid phase is homogeneous. Additionally, as the stirring speed increases, the fluctuation of the liquid surface increases, causing more hydrogen to enter the liquid in the form of bubbles. These giant bubbles break into multiple smaller ones, leading to an increase in the value of a. Moreover, the eddies produced by agitation have a stronger impact on the gas-liquid surface with higher stirring speed, resulting in an increased k_L due to the higher surface renewal frequency (Danckwerts, 1955). Therefore, it is reasonable to observe intensified fluid dynamics in the system with increasing stirring speed, improving the gas-liquid volumetric mass transfer coefficient k_La. Furthermore, the hydrogen dissolution process is endothermic and requires external heating to maintain a stable temperature inside the autoclave. At low stirring speeds (<300 r/min), the heat transfer rate in the PRI-VR is excessively slow, resulting in higher temperatures in the liquid close to the autoclave wall and large temperature gradients inside the autoclave. As a result, the temperature in A_2 fluctuates strongly with hydrogen dissolution in the range of more than 10 °C, which causes a huge error in the pressure data measurement. At high stirring speeds (≥300 r/min), the temperature in A_2 becomes more stable and the pressure data become more accurate.

3.3.2. Effect of pressure and temperature on k_La

As mentioned above, increasing the pressure can enhance hydrogen solubility. To examine the effect of pressure on the mass transfer rate, the k_La values are plotted against the pressure in Fig. 7.

It is revealed that k_La values increase slightly with pressure at a specific temperature and 600 r/min, and the tendency becomes evident as the temperature increases, which is consistent with the literature (Chang and Morsi, 1992; Deimling et al., 1984; Karandikar et al., 1986; Lei et al., 2016). The increase in k_La value with pressure can be attributed to the effect of pressure on the surface tension and viscosity of the solution. As mentioned above, hydrogen solubility increases with pressure, resulting in a decrease in the viscosity and surface tension of the liquid (Chang et al., 1991; Deam and Maddox, 1970), thereby increasing the hydrogen diffusion coefficient. Since the mass transfer coefficient k_L is proportional to the hydrogen diffusion coefficient and inversely proportional to liquid

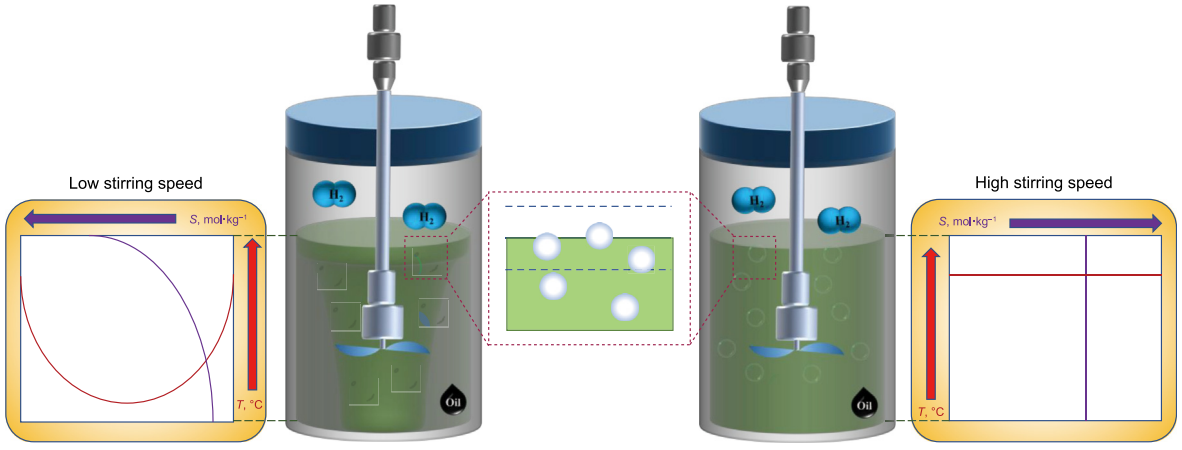

Fig. 6. Effect of stirring speed on gas-liquid mass transfer and temperature of PRI-VR.

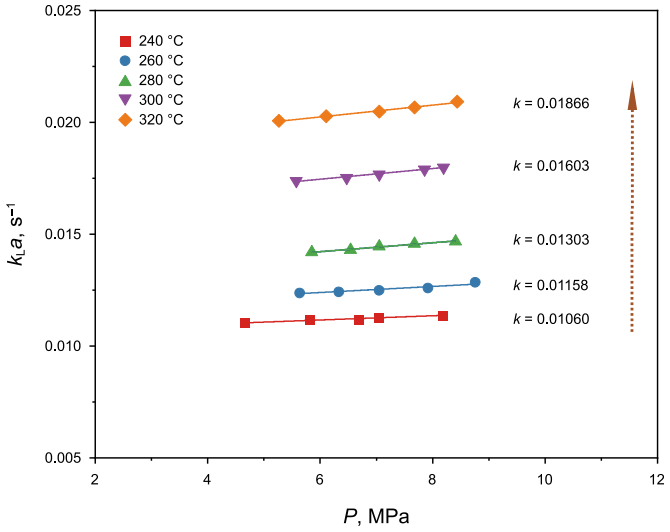

Fig. 7. Volumetric liquid-side mass transfer coefficient k_La at 600 r/min.

viscosity (Tekie et al., 1997), k_L will consequently increase. Additionally, the decrease in surface tension promotes the formation of more bubbles, further increasing the value of a. However, due to the low hydrogen solubility of PRI-VR, the increase in pressure does not significantly improve the physical properties of PRI-VR, resulting in only a subtle positive influence on k_La. Moreover, according to Henry's law, hydrogen solubility becomes more sensitive to pressure as temperature increases, thereby enhancing the effect of pressure on k_La.

Literature comparison has shown that ambiguous results had been obtained regarding the effect of pressure on the values of k_La. The results of Albal et al. (1983) indicated that k_La is independent of pressure in several gas-liquid systems, suggesting an insignificant effect of pressure on bulk and interfacial properties. However, a decrease in k_La with increasing pressure has been reported in the helium-p-xylene system (Teramoto et al., 1974), as confirmed by Chang et al. (1991) in the hydrogen-hexane system. This decrease was attributed to the contraction of bubbles under high pressure and the strengthening of their binding, resulting in a reduction of a in these systems.

Fig. 7 illustrates that the k_La values increase significantly with increasing temperature at a specific pressure and 600 r/min, which is consistent with the literature (Albal et al., 1984; Andersson and Berglin, 1982; Karandikar et al., 1986). The k_La values almost doubled as the temperature increased from 240 to 320 °C. The diffusion coefficient and hydrogen solubility in the residue increase with the temperature, exhibiting precisely the opposite behavior to the viscosity of the residue and surface tension. This opposing trend contributes to a significant increase in k_La. However, reports of a decrease (Deimling et al., 1984; Karandikar et al., 1987) or independence (Joshi et al., 1982; Yoshida et al., 1960) of k_La with increasing temperature have been observed, attributed to the coalescence of foam or bubbles in Fischer-Tropsch liquid at higher temperatures.

Enhancing the volumetric mass transfer coefficient in the hydrogen dissolution system is crucial for the practical application of the residue hydrotreating process on the industrial scale. The enhancement of k_La values can be achieved by increasing temperature and stirring speed, while the effect of pressure is not apparent. Previous studies have confirmed the significant influence of reaction temperature and the slight effect of pressure on the hydrodesulfurization of low-temperature coal tar in the trickle-bed reactor (Feng et al., 2018). It is important to note that the positive contribution of pressure to reaction efficiency primarily stems from its promotional effect on hydrogen solubility. Meanwhile, temperature has a significant influence on both hydrogen solubility and gas-liquid mass transfer. Furthermore, the enhancement of k_La in hydrogen dissolution through stirring speed suggests that process intensification can improve the mass transfer of hydrogen-liquid.

3.4. Gas-liquid mass transfer rate

Fig. 8 shows the dynamic data of hydrogen dissolution using the normalization method for all conditions. As mentioned in Section 2.4, the slope of the S_D-t_D curve is proportional to the mass transfer rate. It reveals that the rate of gas-liquid mass transfer gradually decreases with t_D, irrespective of temperature, pressure, and stirring speed. Furthermore, the gas-liquid mass transfer process remains consistent across all conditions after normalization, despite the significant influence of the operating conditions on hydrogen solubility and equilibrium time.

According to Eq. (5), the difference between the equilibrium concentration of hydrogen in the liquid and the actual concentration of hydrogen in the liquid during the dissolution of hydrogen creates the driving force for gas-liquid mass transfer. As hydrogen continues to dissolve into the liquid, the hydrogen concentration in the PRI-VR increases and gradually approaches hydrogen solubility, thereby reducing the driving force for gas-liquid mass transfer. Furthermore, the hydrogen diffusion rate from the liquid side of the gas-liquid interface into the liquid bulk decreases accordingly, leading to a further decrease in the driving force for gas-liquid mass transfer.

From the above discussion on hydrogen solubility, it becomes evident that PRI-VR has a very low hydrogen solubility due to its composition. This low solubility leads to negligible changes in the physical properties of the liquid even when gas-liquid equilibrium is reached. Consequently, the hydrogen concentration in PRI-VR remains low, and the gas-liquid transfer driving force remains consistently low throughout the gas-liquid transfer process. As a result, there is only a narrow range of rate variation and little difference between the mass transfer rates at any two given moments. Moreover, as the difference between the hydrogen concentration in the liquid and the hydrogen solubility decreases, the gas-liquid mass transfer rate approaches zero. It leads to a relatively time-consuming dissolution of a small percentage of hydrogen before gas-liquid equilibrium. The observed consistency in the rate of dissolved hydrogen, unaffected by experimental conditions after normalization, may be a coincidence resulting from the low mass transfer rate. However, further investigation is needed to fully understand this phenomenon.

The experimental results confirm the significant issue of low gas-liquid mass transfer rates in heavy oils and establish an inverse relationship between the gas-liquid mass transfer rate and the hydrogen concentration in the liquid. Therefore, it is crucial to reduce the concentration of hydrogen on the liquid side of the gas-liquid surface to enhance gas-liquid mass transfer. In the autoclave, increasing the stirring speed enhances the rate of hydrogen transfer from the liquid side of the gas-liquid interface to the bulk of the liquid, as well as the surface renewal rate at the gas-liquid interface. This, in turn, reduces the hydrogen concentration on the liquid side of the gas-liquid interface. Similarly, in the residue HDT using a trickle bed reactor, increasing the gas-to-oil ratio intensifies the gas-liquid mass transfer due to the perturbation caused by hydrogen impinging on the liquid film. These conventional methods lead to the conversion of more gaseous hydrogen into active hydrogen and consequently improve the hydrotreating efficiency of heavy oils. While these approaches offer valuable

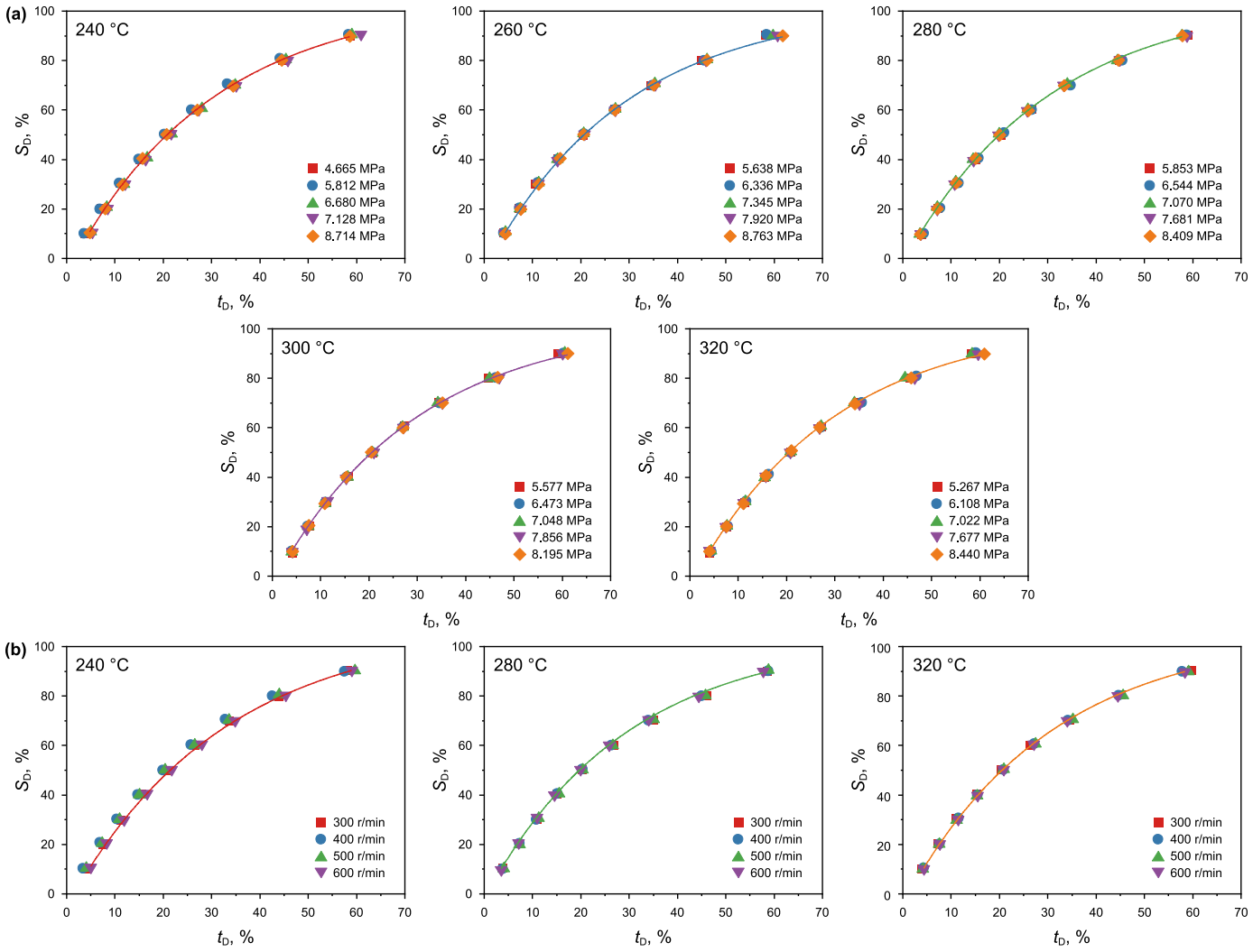

Fig. 8. Variation of mass transfer rate: **(a)** at 600 r/min, **(b)** different stirring speeds.

techniques to enhance mass transfer, the slow gas-liquid mass transfer rate in the hydrotreating process of heavy oils still requires innovative solutions. The results of this study can provide some guidance from the perspective of hydrogen dissolution rate, offering insights for the development of new techniques to address this issue.

4. Conclusion

This study investigates the hydrogen solubility in PRI-VR, as well as the gas-liquid mass transfer rate and its influencing factors, using the modified dynamic pressure step method. The results showed that hydrogen solubility increased with increasing temperature and pressure, in accordance with Henry's law. As the pressure increased from 4 to 9 MPa, the hydrogen solubility roughly doubled. And as the temperature increased from 240 to 320 °C, the hydrogen solubility increased by roughly one-third. The k_La values increased exponentially with stirring speed, which enhanced the mixing of the liquid and increased the surface renewal rate. The k_La values almost doubled with the temperature increase from 240 to 320 °C, which resulted from the increased solubility and diffusion coefficient of hydrogen, as well as the reduced viscosity and surface tension of the liquid. However, the k_La values only slightly increased with pressure, which is due to the weak positive effect of pressure on the physical properties and hydrodynamics of the liquid. Furthermore, the experimental data were normalized, and the results showed that the gas-liquid mass transfer rate gradually decreased during the hydrogen dissolution and that the gas-liquid mass transfer process remained almost the same under all conditions after normalization.

CRediT authorship contribution statement

Tao Jiang: Writing – original draft, Visualization, Validation, Methodology, Data curation, Conceptualization. **Fei Yu:** Data curation. **Qian-Min Jiang:** Data curation. **Yan-Xin Song:** Investigation. **Qing-Feng Tan:** Project administration. **Wu Su:** Project administration. **Xu Yang:** Project administration. **Zhen-Tao Chen:** Writing – review & editing, Project administration, Conceptualization. **Chun-Ming Xu:** Supervision, Formal analysis.

Declaration of competing interest

The authors declare that they have no known competing financial interests or personal relationships that could have appeared to influence the work reported in this paper.

Acknowledgment

This work was financially supported by the National Key R&D Program of China (No. 2022YFB4101300), and National Natural Science Foundation of China (NSFC) (No. 22278430 and 21878329), and Project of R&D Department of CNPC (2020B-2011 and 21-CB-05-05).

Nomenclature

Symbols

C^*	Equilibrium concentration of hydrogen in the liquid
C_L	Hydrogen concentration in the liquid
H	Henry's constant
k_La	Volumetric liquid-side mass transfer coefficient
m_L	Mass of liquid feedstock
N_L	Moles of hydrogen dissolved in the liquid
P_e	Equilibrium pressure of hydrogen dissolution system
P_i	Initial pressure of hydrogen dissolution system
S	Hydrogen solubility
S_D	Normalization of hydrogen concentration in the liquid
t^*	Equilibrium time
t_D	Normalization of dissolution time of hydrogen
T_e	Experimental temperature of hydrogen dissolution system
T_h	Preheating temperature of hydrogen preheating system
V_G	Volume of the gas phase of hydrogen dissolution system
Z_e	Compressibility factor at equilibrium pressure of hydrogen dissolution system
Z_i	Compressibility factor at initial pressure of hydrogen dissolution system

References

Al-Mutairi, A., Marafi, A., 2012. Effect of the operating pressure on residual oil hydroprocessing. Energy & Fuels 26 (12), 7257–7262. https://doi.org/10.1021/ef3011228.

Albal, R.S., Shah, Y.T., Carr, N.L., et al., 1984. Mass transfer coefficients and solubilities for hydrogen and carbon monoxide under Fischer-Tropsch conditions. Chem. Eng. Sci. 39 (5), 905–907. https://doi.org/10.1016/0009-2509(84)85060-5.

Albal, R.S., Shah, Y.T., Schumpe, A., et al., 1983. Mass transfer in multiphase agitated contactors. Chem. Eng. J. 27 (2), 61–80. https://doi.org/10.1016/0300-9467(83)80053-7.

Andersson, B., Berglin, T., 1982. On the theory and use of a new fast-response dissolved hydrogen probe for hydrogen transfer studies. Chem. Eng. J. 24 (2), 201–212. https://doi.org/10.1016/0300-9467(82)80035-x.

Bai, X., Guo, R., Zeng, Z., et al., 2019. Effect of asphaltene contents on hydrogen solubility in heavy oils. CIE J. 70 (10), 4012–4020. https://doi.org/10.11949/0438-1157.20190612.

Baird, Z.S., Uusi-Kyyny, P., Oja, V., et al., 2017. Hydrogen solubility of shale oil containing polar phenolic compounds. Ind. Eng. Chem. Res. 56 (30), 8738–8747. https://doi.org/10.1021/acs.iecr.7b00966.

Brunner, E., 2002. Solubility of hydrogen in 10 organic solvents at 298.15, 323.15, and 373.15 K. J. Chem. Eng. Data 30 (3), 269–273. https://doi.org/10.1021/je00041a010.

Cai, H.Y., Shaw, J.M., Chung, K.H., 2001a. Hydrogen solubility measurements in heavy oil and bitumen cuts. Fuel 80 (8), 1055–1063. https://doi.org/10.1016/s0016-2361(00)00171-x.

Cai, H.Y., Shaw, J.M., Chung, K.H., 2001b. The impact of solid additives on the apparent solubility of hydrogen in petroleum fractions and model hydrocarbon liquids. Fuel 80 (8), 1065–1077. https://doi.org/10.1016/s0016-2361(00)00172-1.

Callejas, M.A., Martínez, M.T., 2000. Hydroprocessing of a maya residue. II. intrinsic kinetics of the asphaltenic heteroatom and metal removal reactions. Energy & Fuels 14 (6), 1309–1313. https://doi.org/10.1021/ef000127+.

Chang, M.Y., Eiras, J.G., Morsi, B.I., 1991. Mass transfer characteristics of gases in *n*-hexane at elevated pressures and temperatures in agitated reactors. Chem. Eng. Process: Process Intensif. 29 (1), 49–60. https://doi.org/10.1016/0255-2701(91)87006-o.

Chang, M.Y., Morsi, B.I., 1991. Mass transfer characteristics of gases in *n*-decane at elevated pressures and temperatures in agitated reactors. Chem. Eng. J. 47 (1), 33–45. https://doi.org/10.1016/0300-9467(91)85005-g.

Chang, M.Y., Morsi, B.I., 1992. Mass transfer in a three-phase reactor operating at elevated pressures and temperatures. Chem. Eng. Sci. 47 (7), 1779–1790. https://doi.org/10.1016/0009-2509(92)85025-7.

Chen, J., Mulgundmath, V., Wang, N., 2010. Accounting for vapor–liquid equilibrium in the modeling and simulation of a commercial hydrotreating reactor. Ind. Eng. Chem. Res. 50 (3), 1571–1579. https://doi.org/10.1021/ie101550g.

Danckwerts, P.V., 1955. Gas absorption accompanied by chemical reaction. AIChE J. 1 (4), 456–463. https://doi.org/10.1002/aic.690010412.

Deam, J.R., Maddox, R.N., 1970. Interfacial tension in hydrocarbon systems. J. Chem. Eng. Data. 15 (2), 216–222. https://doi.org/10.1021/je60045a021.

Deimling, A., Karandikar, B.M., Shah, Y.T., et al., 1984. Solubility and mass transfer of CO and H_2 in Fischer—tropsch liquids and slurries. Chem. Eng. J. 29 (3), 127–140. https://doi.org/10.1016/0300-9467(84)85038-8.

Ding, F.X., Chiang, S.H., Klinzing, G.E., 1985. Hydrogen solubility in coal liquid (SRC-II). Fuel 64 (9), 1301–1305. https://doi.org/10.1016/0016-2361(85)90192-9.

Feng, X., Li, D., Chen, J., et al., 2018. Kinetic parameter estimation and simulation of trickle-bed reactor for hydrodesulfurization of whole fraction low-temperature coal tar. Fuel 230, 113–125. https://doi.org/10.1016/j.fuel.2018.05.023.

Florusse, L.J., Peters, C.J., Pàmies, J.C., et al., 2003. Solubility of hydrogen in heavyn-alkanes: experiments and saft modeling. AIChE J. 49 (12), 3260–3269. https://doi.org/10.1002/aic.690491225.

Heintz, Y.J., Sehabiague, L., Morsi, B.I., et al., 2009. Hydrogen sulfide and carbon dioxide removal from dry fuel gas streams using an ionic liquid as a physical solvent. Energy & Fuels 23 (10), 4822–4830. https://doi.org/10.1021/ef900281v.

Hoekstra, G., 2007. The effects of gas-to-oil rate in ultra low sulfur diesel hydrotreating. Catal. Today 127 (1–4), 99–102. https://doi.org/10.1016/j.cattod.2007.05.001.

Inga, J.R., Morsi, B.I., 1997. Effect of catalyst loading on gasliquid mass transfer in a slurry reactor: a statistical experimental approach. Can. J. Chem. Eng. 75 (5), 872–881. https://doi.org/10.1002/cjce.5450750507.

Ji, S., Wang, Z., Guo, A., et al., 2013. Determination of hydrogen solubility in heavy fractions of crude oils by a modified direct method. J. Chem. Eng. Data. 58 (12), 3453–3457. https://doi.org/10.1021/je400729v.

Jiménez, F., Kafarov, V., Nuñez, M., 2007. Modeling of industrial reactor for hydrotreating of vacuum gas oils. Chem. Eng. J. 134 (1–3), 200–208. https://doi.org/10.1016/j.cej.2007.03.080.

Joshi, J.B., Pandit, A.B., Sharma, M.M., 1982. Mechanically agitated gas-liquid reactors. Chem. Eng. Sci. 37 (6), 813–844. https://doi.org/10.1016/0009-2509(82)80171-1.

Kara, M., Sung, S., Klinzing, G., et al., 1983. Hydrogen mass transfer in liquid hydrocarbons at elevated temperatures and pressures. Fuel 62 (12), 1492–1498. https://doi.org/10.1016/0016-2361(83)90120-5.

Karandikar, B.M., Morsi, B.I., Shah, Y.T., et al., 1986. Effect of water on the solubility and mass transfer coefficients of CO and H_2 in a Fischer-Tropsch liquid. Chem. Eng. J. 33 (3), 157–168. https://doi.org/10.1016/0300-9467(86)80015-6.

Karandikar, B.M., Morsi, B.I., Shah, Y.T., et al., 1987. Effect of water on the solubilities and mass transfer coefficients of gases in a heavy fraction of fischer-tropsch products. Can. J. Chem. Eng. 65 (6), 973–981. https://doi.org/10.1002/cjce.5450650613.

Koneripalli, N., Tekie, Z., Morsi, B.I., et al., 1994. Mass transfer characteristics of gases in methanol and ethanol under elevated pressures and temperatures. Chem. Eng. J. Biochem. Eng. J. 54 (2), 63–77. https://doi.org/10.1016/0923-0467(93)02816-f.

Krishnamurthy, M., Murad, S., Olson, J.D., 2006. Molecular dynamics simulation of Henry's constant of argon, nitrogen, methane and oxygen in ethylene oxide. Mol. Simulat. 32 (1), 11–16. https://doi.org/10.1080/08927020500474318.

Lal, D., Otto, F.D., Mather, A.E., 1999. Solubility of hydrogen in Athabasca bitumen. Fuel 78 (12), 1437–1441. https://doi.org/10.1016/s0016-2361(99)00071-x.

Larachi, F., Cassanello, M., Laurent, A., 1998. Gas-liquid interfacial mass transfer in trickle-bed reactors at elevated pressures. Ind. Eng. Chem. Res. 37 (3), 718–733. https://doi.org/10.1021/ie960903u.

Lei, Z., Dai, C., Yang, Q., et al., 2014. UNIFAC model for ionic liquid-CO (H_2) systems: an experimental and modeling study on gas solubility. AIChE J. 60 (12), 4222–4231. https://doi.org/10.1002/aic.14606.

Lei, Z., Guo, Y., Zhao, L., et al., 2016. H_2 solubility and mass transfer in diesel: an experimental and modeling study. Energy & Fuels 30 (8), 6257–6263. https://doi.org/10.1021/acs.energyfuels.6b00733.

Luo, H., Ling, K., Zhang, W., et al., 2010. A model of solubility of hydrogen in hydrocarbons and coal liquid. Energy Sources, Part A Recovery, Util. Environ. Eff. 33 (1), 38–48. https://doi.org/10.1080/15567036.2010.489106.

Mapiour, M., Sundaramurthy, V., Dalai, A.K., et al., 2009. Effect of hydrogen purity on hydroprocessing of heavy gas oil derived from oil-sands bitumen. Energy & Fuels 23 (4), 2129–2135. https://doi.org/10.1021/ef801005m.

Mapiour, M., Sundaramurthy, V., Dalai, A.K., et al., 2010a. Effects of hydrogen partial pressure on hydrotreating of heavy gas oil derived from oil-sands bitumen: experimental and kinetics. Energy & Fuels 24 (2), 772–784. https://doi.org/10.1021/ef9010115.

Mapiour, M., Sundaramurthy, V., Dalai, A.K., et al., 2010b. Effects of the operating variables on hydrotreating of heavy gas oil: experimental, modeling, and kinetic studies. Fuel 89 (9), 2536–2543. https://doi.org/10.1016/j.fuel.2010.02.024.

Park, J., Robinson, R.L., Gasem, K.A.M., 1996. Solubilities of hydrogen in aromatic hydrocarbons from 323 to 433 K and pressures to 21.7 MPa. J. Chem. Eng. Data. 41 (1), 70–73. https://doi.org/10.1021/je950152n.

Pinos, A.A.R., Badoga, S., Dalai, A.K., et al., 2019. Modelling of H_2 consumption and process optimization for hydrotreating of light gas oils. Can. J. Chem. Eng. 97 (6), 1828–1837. https://doi.org/10.1002/cjce.23450.

Rana, M.S., Sámano, V., Ancheyta, J., et al., 2007. A review of recent advances on process technologies for upgrading of heavy oils and residua. Fuel 86 (9), 1216–1231. https://doi.org/10.1016/j.fuel.2006.08.004.

Riazi, M.R., Vera, J.H., 2004. Method to calculate the solubilities of light gases in petroleum and coal liquid fractions on the basis of Their P/N/A composition. Ind. Eng. Chem. Res. 44 (1), 186–192. https://doi.org/10.1021/ie040056s.

Ronze, D., Fongarland, P., Pitault, I., et al., 2002. Hydrogen solubility in straight run gasoil. Chem. Eng. Sci. 57 (4), 547–553. https://doi.org/10.1016/s0009-2509(01)00404-3.

Saajanlehto, M., Uusi-Kyyny, P., Alopaeus, V., 2014a. Hydrogen solubility in heavy oil systems: experiments and modeling. Fuel 137, 393–404. https://doi.org/10.1016/j.fuel.2014.08.015.

Saajanlehto, M., Uusi-Kyyny, P., Alopaeus, V., 2014b. A modified continuous flow apparatus for gas solubility measurements at high pressure and temperature with camera system. Fluid Phase Equil. 382, 150–157. https://doi.org/10.1016/j.fluid.2014.08.035.

Sebastian, H.M., Lin, H.M., Chao, K.C., 1981. Correlation of solubility of hydrogen in hydrocarbon solvents. AIChE J. 27 (1), 138–148. https://doi.org/10.1002/aic.690270120.

Shaharun, M.S., Mukhtar, H., Dutta, B.K., 2008. Solubility of carbon monoxide and hydrogen in propylene carbonate and thermomorphic multicomponent hydroformylation solvent. Chem. Eng. Sci. 63 (11), 3024–3035. https://doi.org/10.1016/j.ces.2008.02.035.

Sharma, A., Julcour, C., Kelkar, A.A., et al., 2009. Mass transfer and solubility of CO and H_2 in ionic liquid. Case of [bmim][PF6] with gas-inducing stirrer reactor. Ind. Eng. Chem. Res. 48 (8), 4075–4082. https://doi.org/10.1021/ie801584p.

Tekie, Z., Li, J., Morsi, B.I., et al., 1997. Gas-liquid mass transfer in cyclohexane oxidation process using gas-inducing and surface-aeration agitated reactors. Chem. Eng. Sci. 52 (9), 1541–1551. https://doi.org/10.1016/s0009-2509(96)00502-7.

Teramoto, M., Tai, S., Nishii, K., et al., 1974. Effects of pressure on liquid-phase mass transfer coefficients. Chem. Eng. J. 8 (3), 223–226. https://doi.org/10.1016/0300-9467(74)85027-6.

Tsuji, T., Shinya, Y., Hiaki, T., et al., 2005. Hydrogen solubility in a chemical hydrogen storage medium, aromatic hydrocarbon, cyclic hydrocarbon, and their mixture for fuel cell systems. Fluid Phase Equil. 228–229, 499–503. https://doi.org/10.1016/j.fluid.2004.07.013.

Uusi-Kyyny, P., Pakkanen, M., Linnekoski, J., et al., 2017. Hydrogen solubility measurements of analyzed tall oil fractions and a solubility model. J. Chem. Therm. 105, 15–20. https://doi.org/10.1016/j.jct.2016.10.008.

Wang, B., Xiao, C., Li, P., et al., 2018. Hydrotreating performance of FCC diesel and dibenzothiophene over NiMo supported zirconium modified Al-TUD-1 catalysts. Ind. Eng. Chem. Res. 57 (35), 11868–11882. https://doi.org/10.1021/acs.iecr.8b01214.

Wang, B., Zheng, P., Fan, H., et al., 2021. Insights into the effect of solvent on dibenzothiophene hydrodesulfurization. Fuel 287, 119459. https://doi.org/10.1016/j.fuel.2020.119459.

Wang, Z., Chen, S.L., Pei, J., et al., 2014. Insight into the intraparticle diffusion of residue oil components in catalysts during hydrodesulfurization reaction. AIChE J. 60 (9), 3267–3275. https://doi.org/10.1002/aic.14501.

Yoshida, F., Ikeda, A., Imakawa, S., et al., 1960. Oxygen absorption rates in stirred gas-liquid contactors condensed—complete copy for sale. Ind. Eng. Chem. 52 (5), 435–438. https://doi.org/10.1021/ie50605a038.

Zhang, X., Bao, D., Huang, Y., et al., 2014. Gas-liquid mass-transfer properties in CO_2 absorption system with ionic liquids. AIChE J. 60 (8), 2929–2939. https://doi.org/10.1002/aic.14507.

Zieverink, M.M.P., Kreutzer, M.T., Kapteijn, F., et al., 2006. Gas−Liquid mass transfer in benchscale stirred TanksFluid properties and critical impeller speed for gas induction. Ind. Eng. Chem. Res. 45 (13), 4574–4581. https://doi.org/10.1021/ie060092m.